ChemComm

Accepted Manuscript

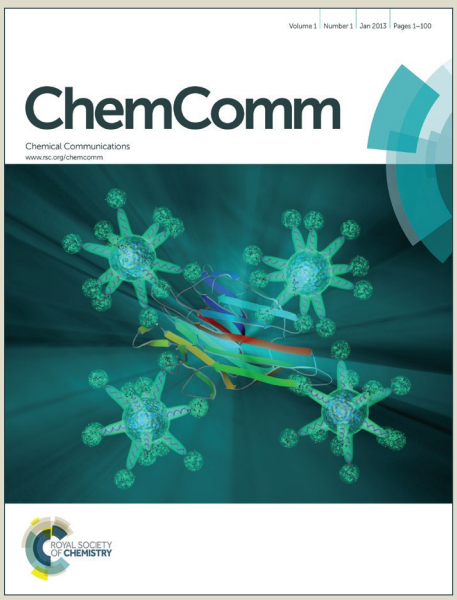

ROYAL SOCIETY OF CHEMISTRY

www.rsc.org/chemcomm

Journal Name

COMMUNICATION

Synthesis and Electrochemical Properties of $Li_{1.3}Nb_{0.3}V_{0.4}O_2$ as a Positive Electrode Material for Rechargeable Lithium Batteries†

Received 00th January 20xx,
Accepted 00th January 20xx

DOI: 10.1039/x0xx00000x

www.rsc.org/

Naoaki Yabuuchi,[a]* Mitsue Takeuchi,[b] Shinichi Komaba,[b] Shinnosuke Ichikawa,[c] Tetsuya Ozaki[c] and Tokuo Inamasu[c]

The binary system, x Li_3NbO_4 – (1 – x) $LiVO_2$, is first examined as an electrode material for rechargeable lithium batteries. The sample (x = 0.43) crystallizes into a cation-disordered rocksalt structure, and delivers reversible capacity of *ca*. 230 mAh g^{-1}, which originates from V^{3+}/V^{5+} redox with electrochemically inactive niobium ions.

The demand for high-energy batteries is further growing after the launch of electric vehicles in the market. Lithium-ion batteries are used as power sources for electric vehicles, and its energy density has been highly increased in the past three decades. Lithium-containing transition metal oxides, such as $LiCoO_2$ and $LiMn_2O_4$, are used as positive electrode materials for lithium-ion batteries. In the past decade, so-called lithium-excess manganese oxides, Li_2MnO_3 and its derivatives, were extensively studied as high-capacity positive electrode materials.[1-6] Li_2MnO_3 with tetravalent manganese ions had been thought to be electrochemically inactive as an electrode material because the oxidation of tetravalent manganese ions into higher oxidation states is difficult. However, the fact is that Li_2MnO_3 is electrochemically active, and its derivatives show an anomalously high reversible capacity with relatively good capacity retention. It has been evidenced that charge compensation is partly achieved by negatively charged oxide ions, instead of transition metal ions, coupled with the conventional redox reaction of transition metal ions.[7, 8]

We have recently reported that Li_3NbO_4 with pentavalent niobium ions is also used as a new host structure for high reversible capacities.[9] Similar to Li_2MnO_3, Li_3NbO_4 is also classified as one of the cation-ordered rocksalt structures. Li_3NbO_4 consists of four edge-shared NbO_6 octahedra (Nb_4O_{16} tetramer) as shown in **Figure 1a**.[10] Lithium ions are accommodated in a body-centered cubic lattice consisting of Nb_4O_{16} tetramers. Although Li_3NbO_4 crystallizes into the lithium-enriched rocksalt structure (lithium to metal ratio reaches three), it is electrochemically inactive because of the absence of electrons in a conduction band ($4d^0$ configuration for Nb^{5+}). Transition metals (Ni^{2+}, Co^{2+}, Fe^{3+} and Mn^{3+}) substituted for Li^+ and Nb^{5+} in Li_3NbO_4 donate electrons in the conduction band. However, the metal substitution results in the formation of a cation-disordered rocksalt structure. Although the formation of the cation-disordered rocksalt structure is expect to be an unavoidable penalty as electrode materials, lithium ions are able to migrate through a percolation network for lithium-excess materials.[9, 11]

In this study, vanadium ions (V^{3+}) are firstly substituted for Li^+ and Nb^{5+} ions in Li_3NbO_4 on the basis of a binary system for x Li_3NbO_4 – (1-x) $LiVO_2$. A single phase is successfully obtained as $Li_{1.3}V_{0.4}Nb_{0.3}O_2$, which corresponds to x = 0.43 in x Li_3NbO_4 – (1 – x) $LiVO_2$. $Li_{1.3}V_{0.4}Nb_{0.3}O_2$ can deliver a large reversible capacity (> 200 mAh g^{-1}) with small polarization for charge/discharge even though the sample crystallizes into the cation-disordered rocksalt-type structure. Its electrode performance is found to be much better than that of $LiVO_2$ with the layered structure. It is evidenced that vanadium ions reversibly are oxidized/reduced based on two electron redox (V^{3+}/V^{5+}) in $Li_{1.3}V_{0.4}Nb_{0.3}O_2$, which is a consistent result with the observed reversible capacity in Li cells.

$Li_{1.3}Nb_{0.3}V_{0.4}O_2$ was prepared by a solid-state reaction from stoichiometric amounts of Li_2CO_3 (>98.5 %, Kanto Kagaku) and Nb_2O_5 (99.9 %, Wako Pure Chemical Industries) and V_2O_3 (98 %, Sigma-Aldrich Japan). The precursors were thoroughly mixed by wet mechanical ballmilling and then dried in air. Thus obtained mixtures of the samples were pressed into a pellet. The pellet was heated at 950 °C for 24 h in inert atmosphere. Thus prepared sample was stored in an Ar-filled glove box until use to avoid oxidation by moist air.

The electrode performance of the sample was examined for the carbon composite sample prepared by ballmilling. As-prepared

[a] Department of Green and Sustainable Chemistry, Tokyo Denki University, 5 Senju Asahi-Cho, Adachi, Tokyo 120-8551, Japan. E-mail: yabuuchi@mail.dendai.ac.jp
[b] Department of Applied Chemistry, Tokyo University of Science, 1-3 Kagurazaka, Shinjuku, Tokyo 162-8601, Japan.
[c] R&D Center, GS Yuasa International Ltd., 1 Inobanba-cho, Nishinosho, Kisshoin, Minami-ku, Kyoto 601-8520, Japan.

† Electronic Supplementary Information (ESI) available: charge/discharge curves of as-prepared sample and a SEM image and XRD pattern of the ball-milled sample (Fig. S1). See DOI: 10.1039/x0xx00000x

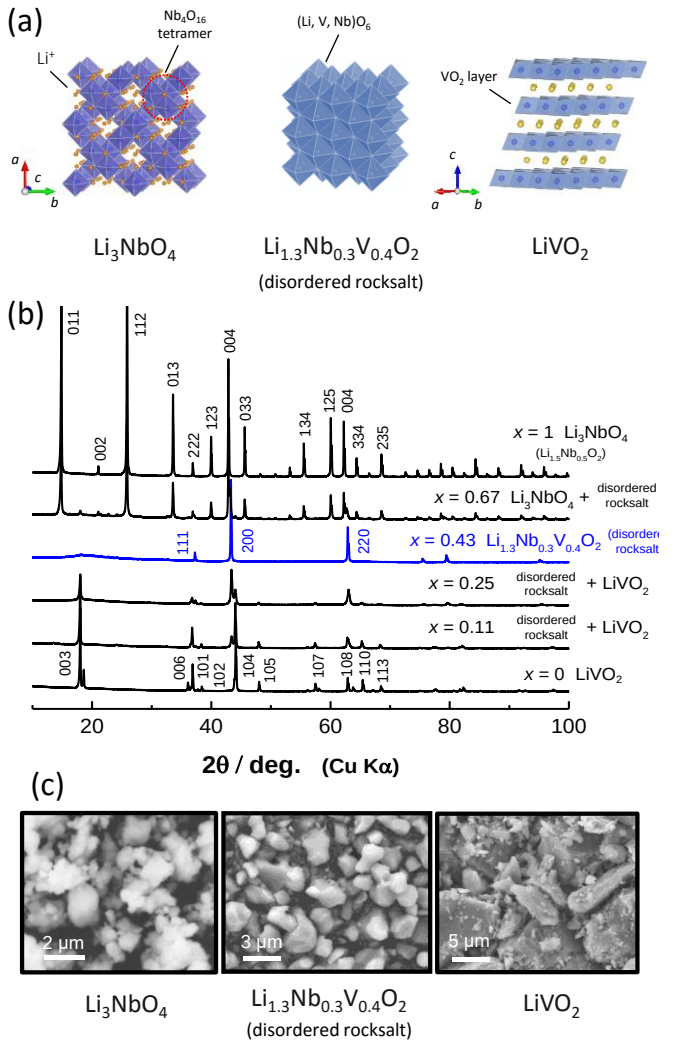

Fig. 1 (a) Schematic illustrations of crystal structures of Li_3NbO_4, $Li_{1.3}Nb_{0.3}V_{0.4}O_2$, and $LiVO_2$. These illustrations were drawn using the program VESTA.[12] (b) X-ray diffraction patterns for the binary system of x Li_3NbO_4 – (1-x) $LiVO_2$. All samples were prepared with the same condition with $Li_{1.3}Nb_{0.3}V_{0.4}O_2$. Particle morphology of Li_3NbO_4, $Li_{1.3}Nb_{0.3}V_{0.4}O_2$, and $LiVO_2$ is compared in (c).

sample was mixed with acetylene black (sample : AB = 80 : 20 in wt%) by using a planetary ballmill (PULVERISETTE 7, FRITSCH) at 300 rpm with a zirconia container and balls. Composite positive electrode consisted of 72 wt% active material, 18 wt% acetylene black and 10 wt% poly(vinylidene fluoride), pasted on aluminium foil used as a current collector. The electrodes were dried at 80 °C in vacuum. Metallic lithium (Honjo Metal) was used as negative electrodes. The electrolyte solution used was 1.0 mol dm^{-3} $LiPF_6$ dissolved in ethylene carbonate : dimethyl carbonate (1 : 1 by volume) (Kishida Chemical). A polyolefin microporous membrane was used as a separator. R2032-type coin cells were assembled in the Ar-filled glove box. The coin cells were cycled in the voltage ranges of 1.0 – 4.2 V or 1.5 – 4.8 V at a rate of 10 mA g^{-1} at room temperature or 60 °C.

Crystal structures of the obtained samples were examined by using an X-ray diffractometer (MultiFlex, Rigaku) equipped with a high-speed position sensitive detector (D/teX Ultra, Rigaku). Non-monochromatized Cu Kα radiation was utilized as an X-ray sou with a nickel filter. The samples were covered with a laboratory mac attachment during the data collection to avoid air exposur Structural analysis was carried out using RIETAN-FP.[13] Schem illustrations of the crystal structure of samples were drawn using th program VESTA.[14] Morphological features of samples were observed using a scanning electron microscope (Carl Zeiss, SUPRA40). Hard X-ray absorption spectroscopy at V K-edge and Nb K-edge was performed at beam line BL-9A of the Photon Factory Synchrotron Source in Japan. Hard X-ray absorption spectra were collected with a silicon monochromator in a transmission mode. The intensity of incident and transmitted X-ray was measured using an ionization chamber at room temperature. Composite electrode samples we prepared using the coin cells at a rate of 10 mA g^{-1}. The composi electrodes were rinsed with dimethyl carbonate, and sealed in water-resistant polymer film in the Ar-filled glove box. Normalizatio of the XAS spectra was carried out using the program code IFEFF The post-edge background was determined using a cubic spline procedure.

X-ray diffraction patterns of the samples for the binary system of x Li_3NbO_4 – (1-x) $LiVO_2$ ($0 \le x \le 1$) are shown in **Figure 1b**. Sing phases of samples are obtained for both end-members, two different cation-ordered rocksalt-type superstructures, Li_3NbO_4 (space grou I-43m) and $LiVO_2$ (space group R-3m), and appearance of a new phase is found in x = 0.43. This new phase, 0.43 Li_3NbO_4 – 0.57 LiV is assigned as a cation-disordered rocksalt structure with a spac group symmetry of Fm-3m. Two phase coexistence, Li_3NbO_4 ar cation-disordered rocksalt, is found in $1 < x \le 0.67$. Similarly, cation disordered rocksalt coexists with $LiVO_2$ in $0 < x \le 0.35$. LiV crystallizes into α-$NaFeO_2$-type layered structure (**Figure 1a**), whic is isostructural with $LiCoO_2$. A single phase region for cation disordered rocksalt seems to be narrow and is found for $0.43 \le x$ 0.5 under the experimental conditions used in this study (950 °C inert atmosphere). The tendency of cation ordering is completely lost for $0.43 \le x \le 0.5$. This phase obtained with x = 0.43 can be reformulated as $Li_{1.3}Nb_{0.3}V_{0.4}O_2$, which has the same oxygen content with the conventional layered structure, $LiMeO_2$. Hereafter, this formulation, $Li_{1.3}Nb_{0.3}V_{0.4}O_2$, is used in this article. A lattice parameter of $Li_{1.3}Nb_{0.3}V_{0.4}O_2$ is calculated to be a = 4.17 Å. Crystal structures of a binary system for x Li_2TiO_3 – (1-x) $LiVO_2$ ($0 \le x \le 1$) a found in the literature.[16] This system crystallizes into the layered structure in the entire range, and formation of cation-disordered rocksalt phase was not evidenced.

Particle morphology of the samples was observed by SEM (**Figure 1c)**. $LiVO_2$ with space group R-3m crystallized into (001) faceted plate-shaped morphology, which is often observed for crystals with layered structures. $LiVO_2$ is easily oxidized in moist air, forming $Li_{1-x}VO_2$ phase for the short time exposure. Such oxidation results in the peak separation of 003 line. A similar result is also reported in $Na_{1-x}VO_2$.[17] Particle morphology changes to round-shaped particles as expected from the cubic symmetry for Li_3NbO_4 (I-43m) and $Li_{1.3}Nb_{0.3}V_{0.4}O_2$ (Fm-3m). The size of primary particles for as-prepared $Li_{1.3}Nb_{0.3}V_{0.4}O_2$ ranges from 1 to 3 μm, which is larger than that of Li_3NbO_4, and the agglomerated secondary particles is not observed

The electrode performance of $Li_{1.3}Nb_{0.3}V_{0.4}O_2$ was examined in Li cells. The as-prepared $Li_{1.3}Nb_{0.3}V_{0.4}O_2$ sample can deliver

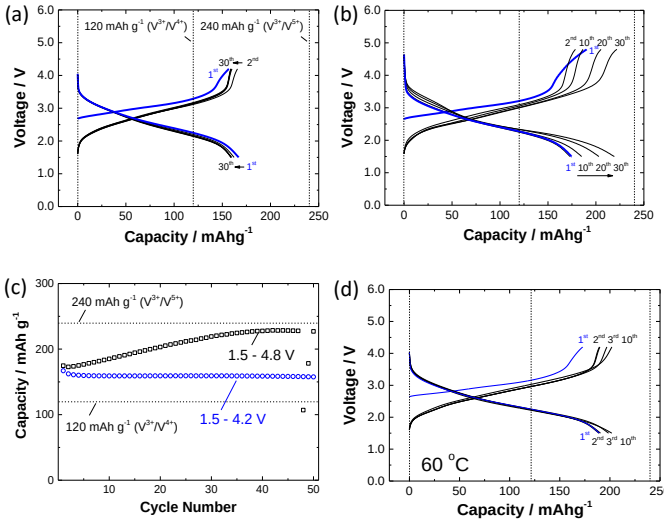

Fig. 2 Galvanostatic charge/discharge curves of $Li_{1.3-x}Nb_{0.3}V_{0.4}O_2$ in Li cells at a rate of 10 mA g^{-1} in the voltage ranges of (a) 1.5 – 4.2 and (b) 1.5 – 4.8 V at room temperature. Discharge capacities for continuous 50 cycles are plotted in (c). (d) Charge/discharge curves of $Li_{1.3-x}Nb_{0.3}V_{0.4}O_2$ in Li cells at a rate of 10 mA g^{-1} in the voltage range of 1.5 – 4.2 V.

approximately 100 mAh g^{-1} of reversible capacity with large polarization of ~0.8 V as shown in **Supporting Figure S1a**. A theoretical capacity of $Li_{1.3}Nb_{0.3}V_{0.4}O_2$ reaches 390 mAh g^{-1} if all lithium ions are reversibly extracted/inserted from/into the crystal lattice. The reversible capacity observed is, however, less than half of 240 mAh g^{-1}, which is consistent with an estimated capacity based on the V^{3+}/V^{5+} two-electron redox process in $Li_{1.3}Nb_{0.3}V_{0.4}O_2$. To reduce particle size and to improve electrical conductivity as a composite electrode, as-prepared $Li_{1.3}Nb_{0.3}V_{0.4}O_2$ (80 wt%) and acetylene black (20 wt%) were thoroughly mixed by mechanical ballmilling. The particle size of $Li_{1.3}Nb_{0.3}V_{0.4}O_2$ is effectively reduced to a sub-micrometer scale and uniformly mixed with nano-sized carbon. A SEM image and XRD pattern of the ball-milled sample are shown in **Supporting Figure S1c**. Electrode performance of the ballmilled sample is shown in **Figure 2**. Reversible capacity as an electrode material is increased and polarization between charge/discharge is effectively reduced by ballmilling (**Supporting Figure S1b**). Polarization as electrode materials is the smallest among the binary system between Li_3NbO_4-$LiMeO_2$ (MeO).[9] The sample can deliver *ca*. 160 mAh g^{-1} of reversible capacity at room temperature in the voltage range of 1.5 and 4.2 V. A sloping voltage profile on charge/discharge is indicative of single phase reaction in the entire range. No capacity degradation is observed for 50 continuous cycles. When the cut-off voltage is raised from 4.2 to 4.8 V, increase in the reversible capacity is observed on the continuous cycles. Reversible capacity observed in the initial few cycles is comparable to that of 4.2 V cut-off, and gradually increases as a function of cycle numbers. After 40 cycles in 1.5 and 4.8 V, reversible capacity reaches *ca*. 230 mAh g^{-1}, which corresponds to 96% of theoretical capacity based on the V^{3+}/V^{5+} redox reaction. The result indicates that an amount of lithium sites, which are connected by percolation network with low penalty for lithium migration, increases on 4.8 V cycles. A study on the origin of increased capacity on 4.8 V cycles is underway in our group. Additionally, kinetics of lithium migration in the percolation network is also enhanced by a rise in temperature. Reversible capacity increases from 160 to 210 mAh g^{-1} for 4.2 V cycles at 60 °C (**Figure 2d**). Similar to $Li_{1.3}Nb_{0.3}V_{0.4}O_2$, Li_2VO_3, which was prepared by electrochemical reduction of $LiVO_3$, is also known as a vanadium-based electrode material with a cation-disordered rocksalt structure.[18] Very recently, fluorinated Li_2VO_3, *i.e.*, Li_2VO_2F, is also proposed as a high-capacity electrode material with vanadium redox.[19, 20] Although nano-sized Li_2VO_2F delivers large initial capacity than $Li_{1.3}Nb_{0.3}V_{0.4}O_2$, much better capacity retention is achieved in this system.

XAS spectra of V and Nb at K-edge were collected for $Li_{1.3-x}Nb_{0.3}V_{0.4}O_2$ with different oxidation/reduction conditions to clarify redox species on oxidation/reduction processes. From V K-edge (mainly dipole transition from 1s core-level to empty 4p level) spectra as shown in **Figure 3a**, energy position of spectra for the as-prepared sample is similar to that of $Li_3V_2(PO_4)_3$ containing trivalent vanadium ions.[21] The spectra clearly shifts to higher energy region as increase in the charge capacity. Additionally, increase in area for a pre-edge peak is found. The strong pre-edge peak mainly originates from an electric dipole transition from 1s to p components, which are hybridized with 3d-orbitals for vanadium ions.[22] Pre-edge peaks by the electric dipole transition are often intensified as decrease in a number of d-orbital electrons.[22] Additionally, electric quadrupole transition from 1s- to 3d-orbitals partially contributes to the pre-edge peak.[23] By considering the observed reversible capacity and change in the profile of V K-edge spectra, trivalent vanadium ions in $Li_{1.3}Nb_{0.3}V_{0.4}O_2$ are oxidized to a higher oxidation state, ~V^{5+}. Note that vanadium ions are reversibly reduced into a trivalent state after discharge to 1.5 V. No change in oxidation states of niobium ions is also found as shown in **Figure 3b**, indicating that niobium ions are not responsible for the large reversible capacity. In addition, on the basis of observed reversible capacity, contribution of oxide ions is not evidenced in the vanadium system. A detailed study on reaction mechanisms is currently in progress and results will be published elsewhere.

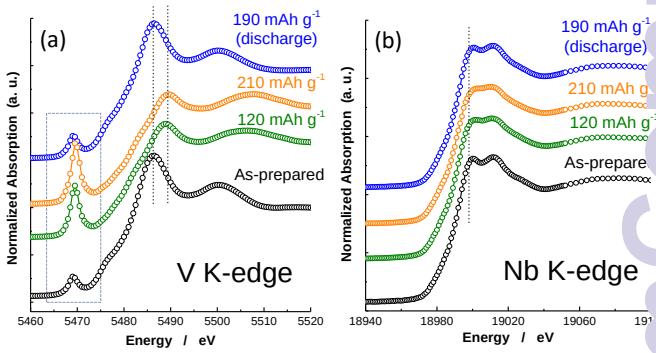

Fig. 3 X-ray absorption spectra at V and Nb K-edges for $Li_{1.3-x}Nb_{0.3}V_{0.4}O_2$ samples: The samples were prepared by electrochemical oxidation in Li cells (charged to 120 and 210 mAh g^{-1}, corresponding to x = 0.4 and 0.7). XAS spectra were also collected after

charge/discharge cycle. The electrode was charged to 210 mAh g^{-1}, and then discharged to 190 mAh g^{-1}.

Conclusions

The binary system, x Li_3NbO_4 – (1 – x) $LiVO_2$, has been first examined as an electrode material for rechargeable lithium batteries. The single phase sample is obtained for x = 0.43 ($Li_{1.3}Nb_{0.3}V_{0.4}O_2$) and the sample crystallizes into cation-disordered rocksalt structure. Lithium ions can migrate in the percolation network coupled with the V^{3+}/V^{5+} redox couple. Furthermore, excellent capacity retention as the electrode material has been confirmed. Capacity loss has been negligible for continuous 50 cycles. These findings will contribute further development of electrode materials with high-capacity and long-cyclability in the future.

Acknowledgments

This study was partly founded by Inoue Foundation for Science. The synchrotron X-ray absorption work was done under the approval of the Photon Factory Program Advisory Committee (Proposal No. 2012G149 and 2012G594).

Notes and references

1. Z. H. Lu, D. D. MacNeil and J. R. Dahn, *Electrochem. Solid State Lett.*, 2001, **4**, A191-A194.
2. Z. H. Lu, L. Y. Beaulieu, R. A. Donaberger, C. L. Thomas and J. R. Dahn, *J. Electrochem. Soc.*, 2002, **149**, A778-A791.
3. A. D. Robertson and P. G. Bruce, *Chem. Mat.*, 2003, **15**, 1984-1992.
4. C. S. Johnson, J. S. Kim, C. Lefief, N. Li, J. T. Vaughey and M. M. Thackeray, *Electrochem. Commun.*, 2004, **6**, 1085-1091.
5. A. R. Armstrong, M. Holzapfel, P. Novak, C. S. Johnson, S. H. Kang, M. M. Thackeray and P. G. Bruce, *Journal of the American Chemical Society*, 2006, **128**, 8694-8698.
6. H. Yamada, W. W. Zhao and H. Noguchi, *Electrochemistry*, 2013, **81**, 460-466.
7. M. Sathiya, G. Rousse, K. Ramesha, C. P. Laisa, H. Vezin, M. T. Sougrati, M. L. Doublet, D. Foix, D. Gonbeau, W. Walker, A. S. Prakash, M. Ben Hassine, L. Dupont and J. M. Tarascon, *Nat Mater*, 2013, **12**, 827-835.
8. M. Oishi, C. Yogi, I. Watanabe, T. Ohta, Y. Orikasa, Y. Uchimoto and Z. Ogumi, *Journal of Power Sources*, 2015, **276**, 89-94.
9. N. Yabuuchi, M. Takeuchi, M. Nakayama, H. Shiiba, M. Ogawa, K. Nakayama, T. Ohta, D. Endo, T. Ozaki, T. Inamasu, K. Sato and S. Komaba, *Proceedings of the National Academy of Sciences*, 2015, **112**, 7650-7655.
10. K. Ukei, H. Suzuki, T. Shishido and T. Fukuda, *Acta Crystallographica Section C*, 1994, **50**, 655-656.
11. J. Lee, A. Urban, X. Li, D. Su, G. Hautier and G. Ceder, *Science*, 2014, **343**, 519-522.
12. K. Momma and F. Izumi, *J. Appl. Crystallogr.*, 2011, **44**, 1272-1276.
13. F. Izumi and K. Momma, *Solid State Phenom.*, 2007, **130**, 1[illegible] 20.
14. K. Momma and F. Izumi, *J. Appl. Crystallogr.*, 2008, **41**, 65[illegible] 658.
15. M. Newville, *J. Synchrot. Radiat.*, 2001, **8**, 322-324.
16. L. Zhang, K. Takada, N. Ohta, M. Osada and T. Sasaki, *J. Power Sources*, 2007, **174**, 1007-1011.
17. C. Didier, M. Guignard, C. Denage, O. Szajwaj, S. Ito, I. Saadoune, J. Darriet and C. Delmas, *Electrochemical and Solid-State Letters*, 2011, **14**, A75-A78.
18. V. Pralong, V. Gopal, V. Caignaert, V. Duffort and B. Raveau, *Chemistry of Materials*, 2011, **24**, 12-14.
19. R. Y. Chen, S. H. Ren, M. Knapp, D. Wang, R. Witter, M. Fichtner and H. Hahn, *Advanced Energy Materials*, 2015, **5**
20. R. Chen, S. Ren, M. Yavuz, A. A. Guda, V. Shapovalov, R. Witter, M. Fichtner and H. Hahn, *Physical Chemistry Chemical Physics*, 2015, **17**, 17288-17295.
21. J. Yoon, S. Muhammad, D. Jang, N. Sivakumar, J. Kim, W.-H. Jang, Y.-S. Lee, Y.-U. Park, K. Kang and W.-S. Yoon, *Journal of Alloys and Compounds*, 2013, **569**, 76-81.
22. T. Yamamoto, *X-Ray Spectrom.*, 2008, **37**, 572-584.
23. F. de Groot, G. Vanko and P. Glatzel, *J. Phys.-Condes. Matter*, 2009, **21**.

TOC